

Breakthrough Propulsion Physics Research at the United States Air Force Academy

Kenneth E. Siegenthaler⁺

Timothy J. Lawrence*

U.S. Air Force Academy Department of Astronautics
Colorado Springs, Colorado

Abstract

The purpose of this paper is to describe research conducted on breakthrough propulsion physics at the United States Air Force Academy. There were two areas of research emphasis, coupling of charge and a rotation mass to produce a force (2 different experiments) and the use of a Heaviside force – coupling of electromagnetic and magnetic fields to produce a force. The possibility of coupling charge and a rotating mass as a means to produce a net force was introduced by Haruo Yamashita in his 1991 European patent application (application number 91310395.8). The basis for this patent is the electrogravitational theory. Allegedly, Yamashita witnessed an eleven gram decrease in weight of his test device, a charged and rotating cylinder. A test device was constructed as closely as possible to Yamashita’s original device. The experiment conducted at the United States Air Force Academy duplicated the experiments Yamashita described in his patents. In addition, additional experiments were performed to further investigate the electrogravitational phenomenon. Although

these experiments produced some interesting results, they failed to duplicate those seen by Yamashita. It cannot be decisively concluded from these experiments that electrogravitation is a real, useful phenomenon.

Nomenclature List

\bar{d}	Difference in Means, General Case
H_a	Alternate Hypothesis
H_o	Null Hypothesis
n	Number of Observations
$n-1$	Degrees of Freedom
s	Standard Deviation, General Case
s_D	Difference in Standard Deviations
t	Test Statistic
$t_{\alpha, n-1}$	Rejection Region
α	Significance Level (0.001)
Δ_0	Test Value (Zero)
μ	Mean, General Case
$\mu_{Neg-Unc}$	Difference in Means for Negative/Uncharged Scenario
$\mu_{Pos-Unc}$	Difference in Means for Positive/Uncharged Scenario

Introduction

Theoretical Background

Electrogravitational theory holds that moving charges are responsible for the mysterious phenomenon we know as

+ Faculty Research Advisor,
Senior Member AIAA
* Faculty Research Advisor

This paper is declared a work of the US Government and is not subject to copyright protection in the United States

gravity. According to Nils Rognerud, author of the paper “Free Fall of Elementary Particles: On Moving Bodies and their Electromagnetic Forces,” gravity as we know it is “...simply a pseudo-force, produced by the special non-shieldable dielectric effect which is produced by the relativistic motions of orbital electrons of ordinary matter”². Much like a moving charge will induce a magnetic field, it will also induce a gravitational field of a much smaller magnitude².

Essentially, according to electrogravitational theory, all gravity is produced by the motion of orbital electrons in the atoms that comprise all matter. This supposed dielectric effect is also additive, unlike the magnetic forces of randomly oriented atoms which cancel each other out². The obvious implication of this statement is that more massive objects, hence possessing more orbital electrons than less massive objects, will produce a greater electrogravitational force. This is a simple explanation of why the earth possesses a stronger gravitational field than the moon, why the sun possesses a stronger gravitational field than the earth, and so on.

Figure 1 is a simple illustration depicting the manner in which a charged particle induces an electrogravitational field. Notice that the produced field is normal to the direction of motion.

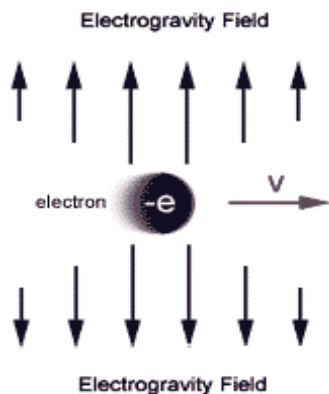


Figure 1. Particle Inducing an EG Field

Figure 2 depicts how an atom produces an electrogravitational field around itself. Again, this field is additive; it becomes stronger with the presence of additional atoms².

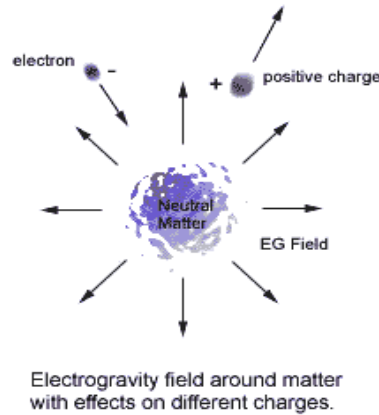


Figure 2. Atom Inducing an EG Field

Electrogravitational theory is much more involved than the brief description provided above. However, this elementary description could be applied to artificially inducing an electrogravitational field.

Experimental Background

By virtue of the assertion that moving particles will induce an electrogravitational field, a charged, rotating cylinder should produce an electrogravity field normal to the plane of rotation. If the cylinder is sufficiently charged and rotating rapidly enough, it should alter its weight in measurable ways. Yamashita attempted this in his 1991 experiment. The result he obtained, an eleven gram reduction in weight of a 1300 gram device, is significant¹. Unfortunately, no one has been able to reproduce his experiment to date. Figure 3 is an illustration of the device that Yamashita had envisioned for the artificial induction of an electrogravitational field.

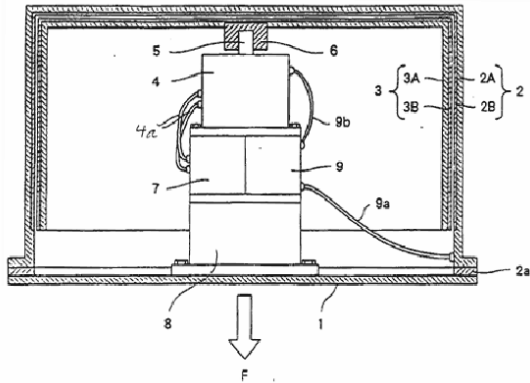


Figure 3. Yamashita's Device

In order to test the validity of his hypothesis, Yamashita constructed a similar device to Figure 3 above that rotated at approximately 50 revolutions per second (3000 revolutions per minute)¹. It was comprised of four main parts: a base plate, an electrode, a rotor, and an electric motor¹. All parts, except the motor, were machined from aluminum¹. The electrode was 130 millimeters in diameter and five millimeters thick¹. It was coated on the interior with a dielectric coating, although Yamashita makes no mention as to what chemicals he used to achieve that purpose¹. The rotor was 127 millimeters in diameter, five millimeters thick, and 60 millimeters high¹. It also was coated with presumably the same dielectric coating, except it was coated on the outside¹. The machine, at rest, weighted 1300 grams¹.

In order to test his machine, he placed it on a scale with a resolution of one gram¹. He tested the machine, uncharged, and rotated it to its maximum speed. The difference in weight between the machine at rest and the machine at this speed was less than one gram¹. Yamashita concluded that there was in fact a difference in weight that his scale could not detect, and he attributed this to the rotor's interaction with the surrounding air¹.

Yamashita applied a charge to his device by bringing into contact the charged Van de Graaf generator's spherical electrode and

machine's electrode for one minute¹. He applied a current of 0.5A to the motor¹. As the rotor accelerated, the scale read increasingly lower weights until at top speed, it read a weight of 1289 grams¹. This represents a decrease in eleven grams, or a one percent decrease in the machine's weight.

Yamashita then reversed the polarity of the rotor. To do this, he attached a spherical electrode to the positive terminal of the generator. He brought into contact the sphere and the machine's electrode, although his patent does not indicate for how long¹. With the polarity reversed, the machine increased its weight by four grams at top speed¹. From this experiment, Yamashita concluded that "horizontal rotation of a charged body generates a vertical force," "when the polarity of the charges supplied to the rotating body is reversed, the direction of the generated vertical force is also reversed," "the faster the body is rotated, the stronger is the generated vertical force," and "the direction and strength of the generated vertical force does not depend on the direction of the body."¹ Yamashita arrived at the last conclusion after his machine produced a force when oriented at an angle¹. Figure 4 depicts Yamashita's experimental setup.

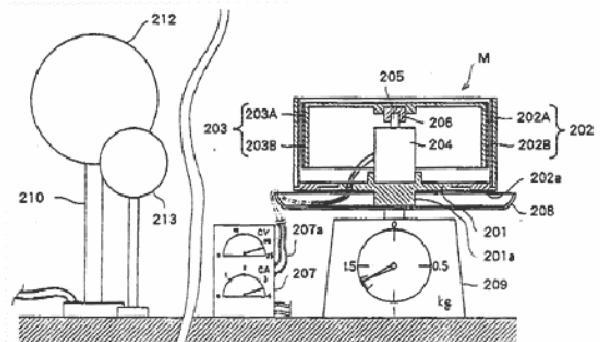


Figure 4. Yamashita's Experimental Setup

No one has been able to reproduce Yamashita's experiments to date. A one

percent decrease in the weight of an object is very significant, and it was the aim of the experiments conducted at the United States Air Force Academy to validate Yamashita's claims and to determine whether or not electrogravitational theory is valid.

Experimental Methods for Experiment #1

Efforts were made to follow Yamashita's experiment as closely as possible. His patent, although somewhat vague, gave enough information to conduct an experiment reasonably true to his original.

The first step in attempting to replicate his experiment was to construct a machine reasonably similar to the one he used. If electrogravitation is indeed a real phenomenon, minor differences between the two machines should not theoretically matter in terms of producing results.

In choosing an electric motor to power the rotor, a Global Super Cobalt 400 27T motor was selected. This motor was originally intended to power radio-controlled aircraft, and it was for this reason that it was chosen to power the replica device. The motor boasts a stall current of 64 amps and is capable of reaching 19,500 revolutions per minute without a load. Compared to most other electric motors, the Global motor is especially powerful and should have no trouble spinning the rotor at speeds higher than those attained by Yamashita's device. Higher speeds, in theory, should induce a larger electrogravitational field that is easier to measure.

A preliminary design was made using Autodesk Inventor Version 7.0. The replica machine was designed specifically for the Global electric motor. For this reason, it is not exactly the same as Yamashita's device. Figure 5 depicts the replica's electrode.

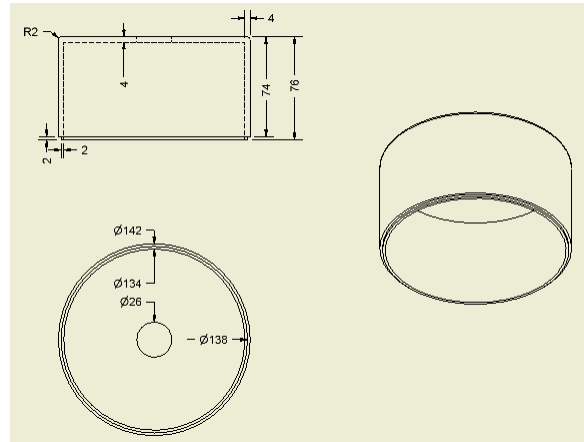


Figure 5. Replica Machine Electrode

Figures 6, 7, and 8 depict the rotor, base plate, and motor mounts, respectively.

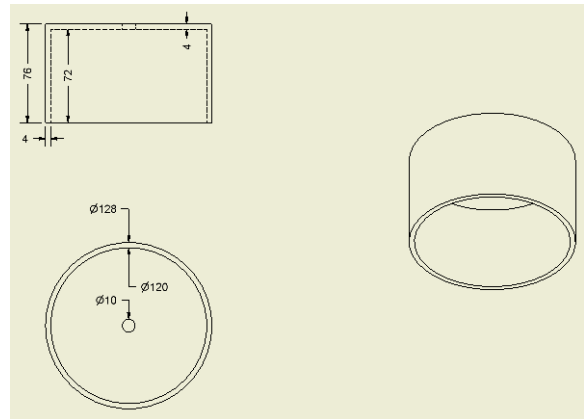


Figure 6. Replica Machine Rotor

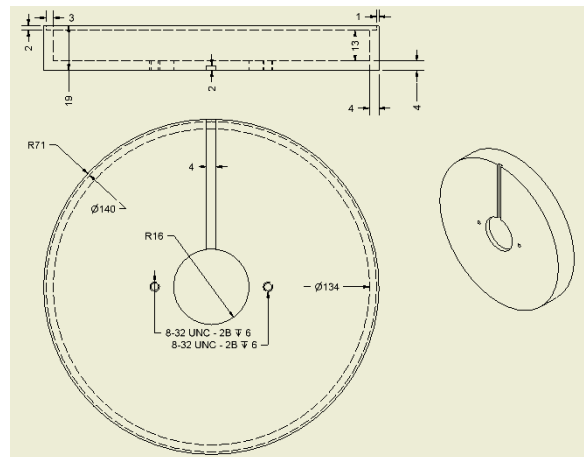


Figure 7. Replica Machine Base Plate

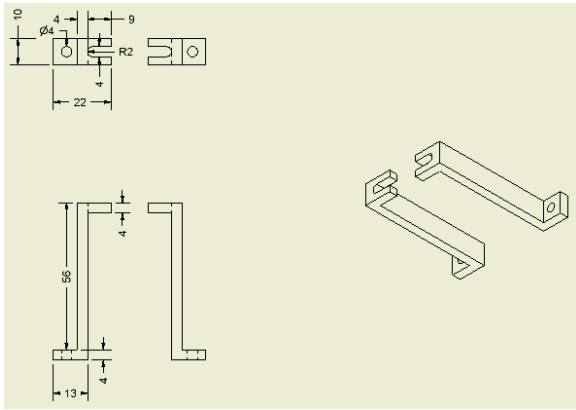


Figure 8. Replica Machine Motor Mount

Yamashita’s machine used an unspecified dielectric material to insulate the electrode from the rotor. Dielectric materials come in many different forms, ranging from gels to baked-on coatings to solid sheets. For the purposes of the replica machine, the surfaces that required a dielectric coating were prepared using one coat of gray automotive primer. To act as the dielectric, four coats of blue enamel paint were applied over the primer. The particular enamel used contained the chemical Xylene, which is known to have a dielectric constant of 2.5 at 25 degrees celsius³. With the dielectric applied, the replica machine was assembled. A specially made nylon washer was used to further insulate the rotor from the motor shaft. Finally, to dampen vibrations, foam padding was applied to the base of the machine.

Figure 9 depicts the appearance of the fully assembled machine.

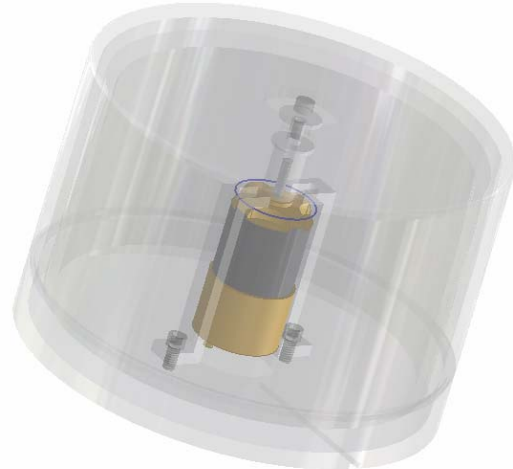


Figure 9. Replica Machine

With the machine fully assembled, a mathematical relationship could be developed between input current and rotor speed. To power the rotor, an Energy Concepts, Incorporated Model 20600B High Current Power Supply was used. Due to the high power requirements of the Global electric motor, a regular power supply could not provide sufficient power to turn the rotor, let alone attain the required rotation rate. On the Model 20600B power supply, the 0-24 Volt setting was selected. The “Amps” setting was then selected to display the supplied current. A vertical line was drawn on the rotor for purposes of speed calibration. A Power Instruments Digistrobe Model M64 strobe light (Calibrated up to 10,000 revolutions per minute) was used in conjunction with the vertical calibration line to obtain the rotor speed. Input current was varied, and the rotor speed associated with that current was recorded. Table 1 shows input currents and the resulting rotor speed.

Input Current (Amps)	Rotor Speed (RPM)
3	500
4	700
4.7	1130
5	1330
5.8	2500

Table 1. Input Current and Rotor Speed

With Table 1, it is relatively easy to develop a function that relates input current to rotor speed using Microsoft Excel. Figure 10 is the Excel graph of Table 1, with rotor speed function shown.

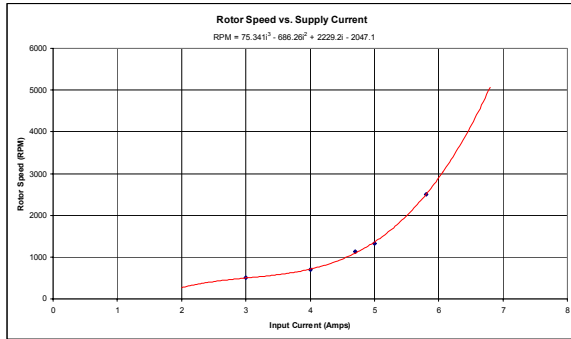


Figure 10. Rotor Speed Graph and Function

The data points fit well on the third order polynomial trendline developed by excel. Equation 1 is the relationship between input current and rotational speed.

$$RPM = 75.341 i^3 - 686.26 i^2 + 2229.2 i - 2047.1 \quad (1)$$

This equation is also shown on the graph. Knowing this equation was necessary. It would not be possible to use a strobe light to monitor the rotor speeds during the test, since the electrode would effectively cover the rotor. It should be noted that the rotor was always spun in a counterclockwise direction. The Global motor is not designed to rotate in the other direction.

To test the replica machine, a thorough, pre-developed test plan was followed. This plan required the use of the Model 20600B power supply to spin the rotor. It also required the use of a Van de Graaf generator to charge the machine. For this purpose, a Wabash Instrument Corporation Winsco Model N-100V generator was used. This particular generator is capable of developing charges

up to 250 kilovolts⁴. Finally, to record the possible weight change, an Ohaus I-10 FE-7000 Precision Scale was used. This particular scale is capable of supporting up to 25 kilograms, with a resolution of one gram. Figure 11 is a photograph of the entire test apparatus, while Figure 12 is a photograph of the machine, the scale, and the power supply.

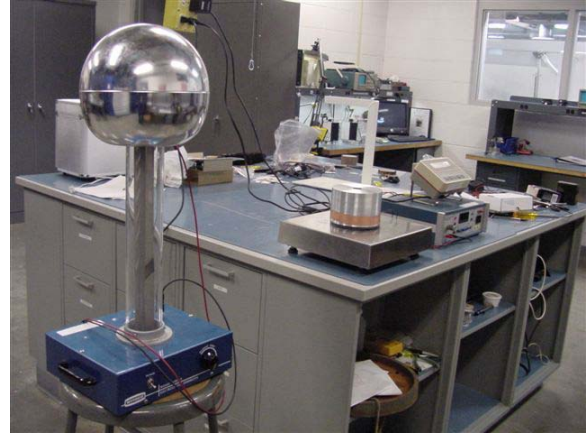


Figure 11. Test Apparatus

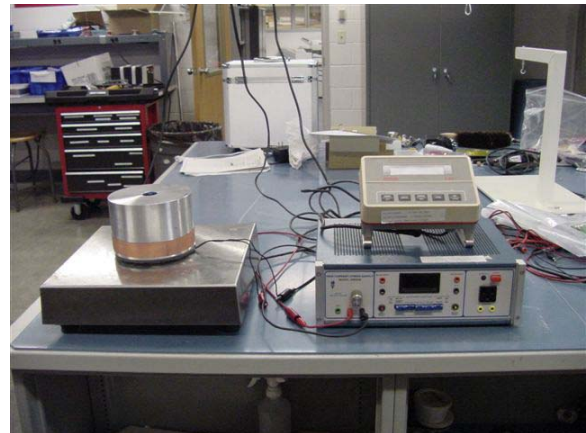


Figure 12. Detail of Machine, Scale, and Power Supply

First, it was necessary to determine whether or not the high levels of static electricity from the Van de Graaf generator had any adverse effects on the scale. To accomplish this, the device was charged for one minute and rotated at full speed in close proximity to the scale. If the reading on the scale

remained constant throughout this process, then it would be assumed that there was no interference.

After establishing that the scale was not affected by the presence of static electricity, the generator was switched off and the machine discharged. The uncharged machine was then placed on the scale. Double sided tape was used to hold the underside of the machine to the scale. This ensured that the machine did not vibrate across the smooth surface of the scale. The wires were placed in such a way that they did not affect the readings on the scale (see Figure 12). Throughout the course of the experiment, the machine would not leave the scale.

Uncharged, the weight of the machine was taken at 500 RPM intervals up to its top speed of 5000 RPM. The purpose of this was to ensure that the machine's vibrations did not cause erratic readings, as well as provide a basis for comparison for charged operation. After this test, the machine was allowed to come to a complete stop.

The next test involved charged operation. The machine was charged for one full minute from the Van de Graaf generator. A wire was used to connect the spherical electrode of the generator to the electrode on the machine. After the machine was fully charged, the Van de Graaf generator was switched off and grounded to ensure it carried no residual charge that might have caused interference. As was the procedure of the previous test, the weight of the machine was recorded at 500 RPM intervals, from zero to 5000 RPM. At these intervals, the machine's weight was recorded.

Afterwards, the machine was allowed to stop and was discharged. The Van de Graaf generator was again used to charge the

machine. This time, however, contact was made through a wire from the generator's positive electrode on its base to the machine's electrode for one full minute. The previous test was again conducted, this time with the opposite charge, and the weight values were recorded.

The next series of tests involved testing, at full speed, various levels of charge and their effects on the machine's weight. Using the same procedures previously described for charging, the machine was charged in ten second intervals, ranging from 10 to 60 seconds, from the negative spherical electrode of the generator. At each of these charge intervals, the machine operated at full speed, and its weights were recorded. Between each charge interval, the machine was allowed to come to a complete stop and be fully discharged. For example, the first step of this test involved charging the machine for 10 seconds. It was then tested, stopped, and discharged. The second step involved charging the machine for 20 seconds and repeating the same process. The third step involved charging the machine for 30 seconds, and so on, until the machine received one full minute of charging. Finally, this same test was conducted with the machine receiving a positive charge from the electrode on the base of the generator.

It was hoped that by following these procedures that Yamashita's claim would be validated. Furthermore, it is hoped that by using more thorough procedures, electrogravitational theory can either be validated or rejected.

Results and Discussion of Experiment #1

Although not conclusive by any means, the results of this experiment were nonetheless interesting. By operating the fully charged

machine in close proximity to the scale, it was determined that the static electricity had no adverse effect on the other equipment, especially the scale.

The first test involved the uncharged machine at various speeds. Table 2 contains the input currents, associated speeds, and weights of the machine.

Supply Current (A)	Rotor Speed (RPM)	Machine Weight (g)
0.0	0	1315
3.0	500	1315
4.6	1000	1315
5.1	1500	1315
5.5	2000	1315
5.8	2500	1316
6.0	3000	1316
6.3	3500	1316
6.5	4000	1316
6.6	4500	1316
6.8	5000	1316

Table 2. Uncharged Rotation, Speed Varied

As the rotor was accelerating, the scale fluctuated at ± 2 grams above and below the central value. When the rotor reached a steady speed, the fluctuation in some cases disappeared; in others was ± 1 gram about the central value. In these cases, it was the central value that was recorded as the machine's weight. These fluctuations for the most part seemed to be caused by the natural vibrations in the machine, although the rotor's interaction with the surrounding air plays a part as well.

The next test involved varying rotor speed with a full negative charge. Table 3 contains the test data from this scenario, as well as the differences in weight between the present and the uncharged test cases.

Rotor Speed (RPM)	Machine Weight (g)	Weight Change (g)
0	1315	0
500	1315	0

1000	1315	0
1500	1315	0
2000	1315	0
2500	1315	-1
3000	1315	-1
3500	1314	-2
4000	1314	-2
4500	1314	-2
5000	1314	-2

Table 3. Negative Charge, Speed Varied

The next test involved varying rotor speed with a full positive charge. The data for this scenario is listed in Table 4, again, showing the change in weight from the uncharged test case.

Rotor Speed (RPM)	Machine Weight (g)	Weight Change (g)
0	1315	0
500	1315	0
1000	1315	0
1500	1316	+1
2000	1316	+1
2500	1316	0
3000	1316	0
3500	1316	0
4000	1316	0
4500	1317	+1
5000	1317	+1

Table 4. Positive Charge, Speed Varied

The next test involved varying negative charge at full rotational speed. Table 5 lists the resulting data.

Charge Time (sec)	Machine Weight (g)	Weight Difference (g)
0	1315	0
10	1315	-1
20	1315	-1
30	1315	-1
40	1314	-2
50	1314	-2
60	1314	-2

Table 5. Constant Speed, Varied Negative Charge

After obtaining the data for the 60 second charge time at full speed, the machine broke.

An inaccessible screw holding the motor to the motor bracket came loose, and with no way to adequately tighten it, the machine would vibrate violently above 500 RPM. At this point, enough data had been taken; the constant speed, varying positive charge test was scrubbed.

Enough data had been acquired to statistically test whether or not this experiment offered proof that electrogravity was indeed a real phenomenon. Even though there was an apparent decrease in weight through negatively charged rotation and an increase through positively charged rotation (as Yamashita had predicted), it may not have been a measurable enough of a change to reach a definite conclusion.

The varied rotation speed with one minute charge will be of statistical interest. The uncharged rotation will be used as a basis for separate comparison between the negative and the positive charged cases. This data will be considered paired data, since it consists of two observations on the same unit, that unit being speed of rotation. Consequently, a *t*-test will be used. The null hypothesis, in this case, is that there is no difference between the mean weight of the uncharged scenario and that of whatever it is being compared to, either the positive or negative. On the contrary, the alternative hypothesis holds that there is a difference in the means. The *t*-test will be used to either reject or accept the null hypothesis. Rejection of the null means that it is statistically sound to accept electrogravitational theory based on the experimental data. Accepting the null signifies the opposite, or the experimental data is statistically insufficient to prove the existence of an electrogravitational force.

Table 6 shows all pertinent data for statistical analysis of the negatively charged case.

	Uncharged	Negative	Difference
μ	1315.5455	1314.636364	-0.90909
s	0.522233	0.504524979	0.94388

Table 6. Negative Charge Statistical Data

The two hypotheses in this case are as follows:

$$H_0: \mu_{Neg-Unc} = 0$$

$$H_a: \mu_{Neg-Unc} < 0$$

(2)

For this analysis, a significance level of $\alpha = 0.001$ will be used. Furthermore, there are a total of $n = 11$ observations. For this test, the test statistic will be as follows:

$$t = \frac{\bar{d} - \Delta_0}{s_d / \sqrt{n}}$$

(3)

This test statistic will be compared to $t_{0.001,11-1} = 4.144$. If the following relationship is found to be true, then H_0 will be rejected.

$$t < -t_{\alpha,n-1}$$

(4)

Stepping through all of the math for the comparison of the uncharged and negatively charged data, the following is found to be true:

$$t = \frac{-0.90909 - 0}{0.94388 / \sqrt{11}} = -3.194$$

(5)

This particular test value, when compared to $t_{0.001,11-1} = 4.144$, makes equation 4 false.

Therefore, it is necessary to fail to reject the null hypothesis. The experimental data for the negative case is insufficient to prove the existence of an electrogravitational force.

The same test must be performed between the uncharged and the positively charged scenarios. Table 7 contains all the necessary data for this comparison.

	Uncharged	Positive	Difference
μ	1315.5455	1315.909091	0.363636
s	0.522233	0.70064905	0.8202

Table 7. Positive Charge Statistical Data

Unlike the previous case, this case requires a different set of hypotheses. H_a must be the opposite for this case, since positive rotation tended to cause the machine to gain weight rather than lose weight. The set of null hypotheses required for this test are as follows:

$$H_0: \mu_{Pos-Unc} = 0$$

$$H_a: \mu_{Pos-Unc} > 0$$

(6)

Likewise, the test relationship shown in equation 4 must be changed. The test relationship now becomes:

$$t > t_{\alpha, n-1}$$

(7)

Using equation 5 to obtain the test statistic,

$$t = \frac{0.363636 - 0}{0.8202 / \sqrt{11}} = 1.470$$

(8)

Using $t_{0.001,11-1} = 4.144$ as in the previous case, equation 7 is not satisfied. Therefore H_0 must be accepted in this case also. There is not enough evidence from the experimental data from the positive case that electrogravity is a real force. Statistical analysis of the varied charge test is not necessary. The analysis performed on the initial data proves that the experimental data is not sufficient to confirm the existence of an electrogravitational force.

Experimental Methods for Experiment #2

After the results obtained in Experiment #1, another attempt was made to replicate the results and make improvements. However, funding issues precluded the implementation of a key improvement. This was conducting the experiment in a vacuum environment. After several inquiries to different electric motor manufacturers, it was found that a vacuum rated motor capable of spinning the rotor at the desired RPM would cost roughly \$1000. Additionally, the manufacturers would not be able to supply a motor in a fashion which would meet the timetable requirements of this paper. Many of the motors were out of stock or would have to be custom-made for the purposes of this experiment. This postponed the arrival of a motor by several months, precluding their use even if funding was available.

Another objective of the second experiment was to investigate the reason why the previous experiment's machine failed at high speeds. The rotor used in the previous machine was plagued with balancing issues. These were first believed to have come from painting the rotor, however further investigation led to the conclusion that last years rotor was in fact out of balance without the paint and that the hole drilled for the motor shaft interface was out of center. Additionally, the motor mount previously

designed was determined to be insufficient to keep the machine stable at high RPMs, especially given the imbalanced rotor. This conclusion was reached through inspection of the motor mount when fully assembled and attached to the base plate and motor. The motor mount was comprised of only two brackets which were attached to the motor and base plate with a total of 4 screws as illustrated in Figure 8. The motor mount was also attached to the motor with hot glue. The motor used was also in question as the slender shaft of the motor may have contributed additional instabilities of the experiment at high speeds.

Another discrepancy found was that the electrode did not fully enclose the rotor – there was a hole at the top which provided access to a screw which held the rotor to the motor interface. Whether or not this hole would have affected experimental results has not been determined, but it can be hypothesized that such a hole could introduce a larger possibility for aerodynamic effects as opposed to a completely enclosed and sealed device. A figure of the previous year’s electrode and Yamashita’s device can be seen in Figures 3, 4 and 5. From Yamashita’s drawings, it is seen that neither iteration include a hole in the electrode component.

The experiment was conducted as closely as possible to Yamashita’s experiment; however the ambiguity of the European patent application led to educated guesses on a few aspects during the design of the machine. In addition, accuracy limitations of the manufacturing tools at the Air Force Academy introduced errors to the components, more specifically the rotor. These ambiguities and limitations led to many iterations of the machine while in the construction phase of the experiment. The initial design for the machine can be seen in

the figure on the next page, but the final iteration of the machine differed greatly from this drawing. The final version of the machine is shown later in the paper.

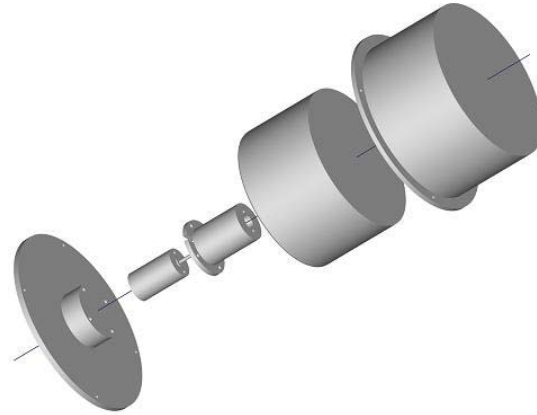


Figure 13. Initial Design of the Machine.

An enlarged view of the new motor mount design can be seen in the following figure. It can be seen that this design would be much more stable than the two-bracket design from the previous machine, however implementation of this motor mount was not allowed given issues with the motors detailed later in the paper.

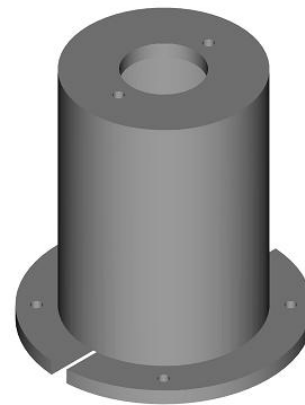


Figure 14. Motor Mount.

Given the criticality of accuracy in manufacturing the components, the tools used were integral in allowing the components to meet exacting standards, however it was determined that the facilities at the Air Force Academy were not capable

of machining within such tolerances. The limitations present were a great hindrance, especially in manufacturing the rotor. The rotor that was manufactured for this year's machine was out of balance in addition to being out-of-round. The out-of-roundness of the rotor was mainly due to how thin the aluminum was. When compared to last year's rotor (mounted on this year's machine) the vibrations experienced by the new rotor were much greater, therefore last year's rotor was reused in this experiment. In addition it was shortened to reduce the mass moment of inertia values. The same thickness was kept to maintain the durability of the rotor.

After analysis of the previous experiment's motor, it was hypothesized that the motor shaft was bent, contributing to the vibrations experienced. Three different motors were tested with the old rotor and each experienced similar vibration. Although specific dimensions of the motor and motor shaft were not provided in Yamashita's patent application, further investigation of his drawings led to the conclusion that a motor with a very thick shaft was used in his experiment, therefore a shaft diameter of about 0.25 in was decided upon. Furthermore a thicker shaft would bolster the stability of the spinning rotor given how imbalanced it was. Hobby shops did not provide motors with a shaft thickness in the range of 0.25 in, therefore more creative means were employed to find a desirable motor. A 130 VAC brushless electric fan motor with a shaft thickness of 6 mm (slightly under 0.25 in) was found at a Goodwill store. To power the motor, an Energy Concepts, Incorporated Model 20600B High Current Power Supply was used.

The fan cover and blades were removed leaving only half of the fan casing, the

motor, speed control, and stand. The integrated speed control of the fan was set to maximum for the entire experiment. A picture of that assembly can be seen in Figure 15.



Figure 15. Modified Fan.

Given the peculiar method that the motor was mounted to the fan assembly, it would have been difficult and time consuming to design and build a new mount for the fan motor, therefore it was decided that the base plate would be mounted on top of the fan motor with the shaft protruding from the bottom of the base plate. This is illustrated in Figure 16.



Figure 16. Base Plate Mounted on Fan.

Since the design had gone through several iterations at this point, different sets of holes

had been placed on the base plate. After initial construction it was determined that these should be covered with aluminum tape to mitigate airflow through this section.

Additionally the motor mount interface posed a problem as it presented more opportunities for inaccuracies to be introduced. The previous year's rotor-to-motor interface was held to the motor shaft by friction fit, but after many uses this interface became loose. Another method of interfacing the motor to the rotor was improvised by using a small hand drill chuck to clamp on to the motor shaft. Running the motor at maximum speed with the chuck attached produced minimal vibrations. Further detail as to how these components were interfaced is illustrated in the Figure 17.



Figure 17. Drill Chuck on Motor Shaft.

A reference line was drawn on the chuck, then using a strobe light rated to over 18000 RPM and the Model 20600B placed on the 130 VAC setting, the maximum rotational speed of the motor was determined to be roughly 3390 rpm. Though this was much slower than the previous year's maximum speed, it was sufficient to meet the specifications detailed in Yamashita's experiment. The method of determining the rotational speed of the rotor in relation to the

current supplied was identical to the previous experiment and is further elaborated later in the paper. The rotor-to-motor interface was attached to the chuck via screw. Since the previous experiment's interface produced minimal vibrations when attached to the motor it was also reused for this experiment; however it was re-drilled and tapped to hold a screw that fit into the chuck. The interface was attached to the rotor via two countersunk screws which completed the assembly for attaching the rotor to the motor shaft. Although much more complex, when fully assembled the rotor spun with less vibration than the previous year's machine. Unfortunately at high speeds these vibrations were still apparent. The final assembly is illustrated in Figure 18.



Figure 18. Rotor Mounted on Shaft.

The vibrations were mitigated through manually balancing the rotor. The rotor had to be manually balanced because machine shops which offered professional balancing services were not able to fit the rotor on their balancing machines as the shaft size for the motor was too thin. A shop was found which was able to balance rotors with smaller shaft sizes (specifically turbochargers for cars), but this development occurred too late in the manufacturing process to meet deadline requirements.

Given that the hole drilled for the interface was off center, a micrometer was used to determine the point on the rotor with the smallest radius. Additional mass was added to this point by attaching solder to the inside of the rotor with aluminum tape. This addition greatly minimized the vibrations of the rotor, especially at high speeds. Fine tuning of the rotor's balance was achieved through an iterative process of adding a mass (section of 18 gauge wire attached with duct tape), spinning up the motor to its maximum velocity, judging whether the addition decreased the total vibration of the machine, and moving the mass to a new location. Locations with the least vibration were marked, compared, and the optimum location of the additional mass was determined through observation. After several masses were added to the rotor (all on the inside surface), it became increasingly difficult to judge the differences in severity of vibration. At this point it was considered that the rotor was balanced to the maximum extent possible given the method implemented.

Once the rotor was balanced, it was painted and retested to see if the paint had any noticeable affects. Since Yamashita's patent application did not specify the exact dielectric layer used, for this experiment Vanguard Class F Red VSP-E-208 Insulating Enamel was utilized to insulate the inner surface of the electrode and the outer surface of the rotor. This insulating enamel is specifically designed to insulate electrical components. To ensure an even coating on the outside of the rotor, the paint was applied as the rotor was spinning. When applied the paint did not have any adverse affects on the balance of the rotor. Once the paint was applied, a calibration curve which related rotor speed to applied current was developed using the strobe light

and by making a reference line on the rotor. The results can be seen in Table 8.

Amps	RPM
0.20	621
0.21	1983
0.22	2860
0.23	3015
0.25	3165
0.30	3277
0.35	3330
0.40	3350
0.45	3368
0.50	3377
0.60	3385
0.74	3390

Table 8. Relation of Amps to RPM

From the data in Table 8 a linear regression between each point was derived using the "TREND" function in Microsoft Excel. This function determined the RPM associated with intermediate levels of current. The "TREND" function was used between each point because the regression lines that Excel produced did not match well with the data. Figure 19 is a graph of the data points from the Table 8.

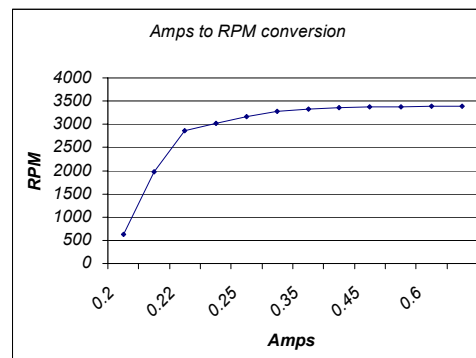


Figure 19. Graph of Amp to RPM Conversion.

A relation between current and RPM was required because the rotor would not be visible once the electrode was attached.

When connecting the electrode to the assembly, Styrofoam was used as an insulative layer to separate the electrode from the base plate. Nylon screws were used to hold the two components together. The final assembly of the device can be seen in Figure 20. Though the internal components of the machine were exposed, the aerodynamic effects generated by the spinning rotor were minimal as detailed in the results later in this paper.



Figure 20. Machine Fully Assembled.

To measure the weight change a Mettler PM6100 scale was used. Provided by the Chemistry Department, this scale had a resolution and range of 0.01 g and 6100 g respectively. The scale was grounded with a 28 gauge wire in order to protect the equipment from static discharge. This wire was oriented in such a way that it would not affect the weight of the machine and is illustrated in Figure 21.



Figure 21. Wire used to Ground the Scale.

A Wabash Instrument Corporation Winsco Model N-100V Van de Graf generator was provided by the Physics department and used to charge the machine. The Van de Graf generator's spherical electrode was attached to the machine's electrode via wire. Although Yamashita's patent application depicted charging the machine's electrode by directly touching it with the Van de Graf generator's electrode, the sensitivity of the scale utilized precluded the implementation of that procedure. Instead a wire was used to connect the generator's electrode to the machine's. The procedures for the experiment are as follows:

With the power supply and the charge supply off, the weight of the machine was measured. The wire for the motor was oriented in such a way that they would not affect the weight of the machine. This was also true for the wire used to charge the machine. These are illustrated in the following figures. The mass measurement was made several times while shaking the wires connected to the motor and power supply, and mass differences less than 0.1g were observed. Given the results of shaking the wires, they would need to be kept still during experimentation.

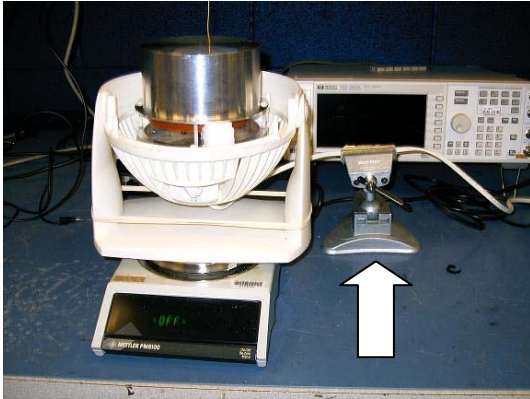


Figure 22. Clamp Holding Motor Cord.

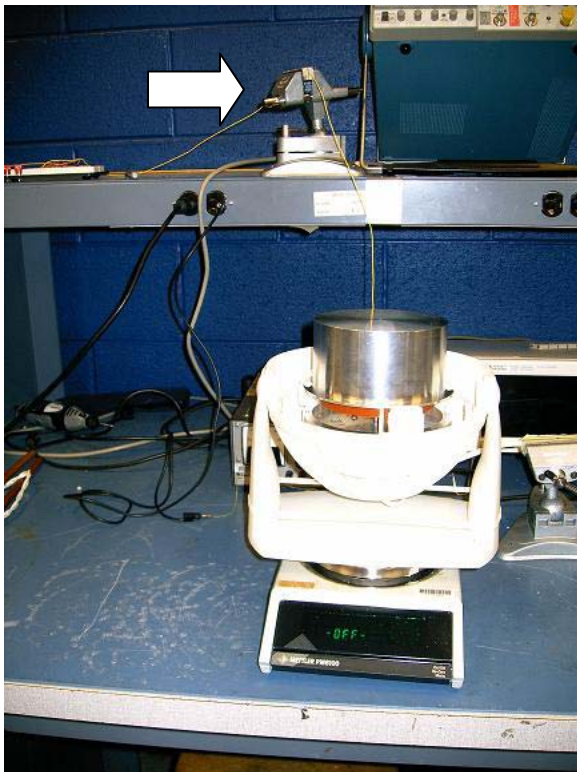


Figure 23. Clamp Holding the Charging Wire.

The power supply was then turned on, and the rotor was accelerated rapidly. From the acceleration test it was seen that the machine's mass would fluctuate by less than ± 0.1 grams if maximum current were applied at rest. Further testing indicated that a current increase of 0-0.74 Amps in 60 seconds produced (relatively slow acceleration) smaller fluctuations in mass. It

was then decided that the rotor would be allowed to run at determined Amp levels for ten seconds before proceeding to further accelerate the rotor. Increasing the current by 0.05 amps and allowing the rotor to spin at the Amp level for ten seconds, the mass readings were recorded.

To check whether the electrode held charge, the machine was connected to the Van de Graf generator via wire, which can be seen in Figure 24. The generator was then turned on and allowed to charge the electrode for one minute. After one minute the generator was disconnected from the electrode and turned off. The device illustrated in Figure 25 was then connected to the ground socket in a wall outlet and brought within close proximity of the electrode. A spark was observed, verifying that the electrode had been charged by the generator.

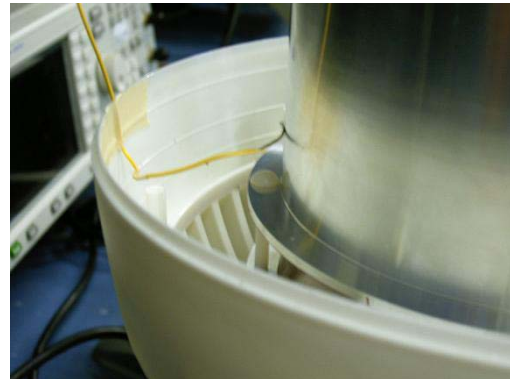


Figure 24. Wire Connecting the Van de Graf Generator to the Electrode.



Figure 25. Device Used to Check Charge.

Then with the rotor at rest, the Van de Graf generator was turned on and reconnected to the machine's electrode. After one minute of charging the electrode, the wire was disconnected from the machine's electrode and the Van de Graf generator was taken to the other side of the room and turned off.

The rotor was then accelerated to its top speed, taking readings of the scale at intervals of 0.05 Amps, remaining at each level for ten seconds. These procedures were then repeated with the positive terminal of the Van de Graf generator charging the electrode. A third test was also performed with the generator attached to and continually charging the machine at a low rate while the rotor accelerated.

Results and Discussion of Experiment #2

When uncharged, the difference in mass between 0 RPM and 3390 RPM was less than 0.02 g. This difference can be considered to be caused by an interaction between the rotor rotation and the surrounding air as the machine was not fully enclosed. Additionally, the slight vibrations which resulted from the machine's operation may have caused these fluctuations given the scale's sensitivity. Table 9 depicts the mass fluctuations when accelerating the uncharged electrode.

Amps	RPM	Mass (g)	Change (g)
0	0	2585.01	0
0.21	1983	2585.02	0.01
0.24	3087.764	2585.01	0
0.29	3254.6	2585	-0.01
0.34	3319.4	2585.01	0
0.39	3346	2585.02	0.01
0.44	3364.4	2585.01	0
0.49	3375.2	2585.01	0
0.54	3380.2	2585.01	0
0.59	3384.643	2585.00	-0.01
0.64	3386.429	2585.01	0
0.69	3388.215	2585.02	0.01
0.74	3390	2585.01	0
0	0	2584.99	-0.02

Table 9. Uncharged Operation

It is seen from the data that the machine's mass stays fairly constant while accelerating, indicating very smooth operation; however the small fluctuations that do occur may have been caused by slight interference from either air or small vibrations from the machine itself.

When charging the electrode using the negative terminal of the Van de Graf generator, the scale produced the mass changes illustrated in Table 10.

Amps	RPM	Mass	Change
0	0	2584.99	0
0.21	1983	2584.99	0
0.24	3087.764	2584.99	0
0.29	3254.6	2584.98	-0.01
0.34	3319.4	2584.98	-0.01
0.39	3346	2584.99	0
0.44	3364.4	2584.97	-0.02
0.49	3375.2	2584.97	-0.02
0.54	3380.2	2584.97	-0.02
0.59	3384.643	2584.99	0
0.64	3386.429	2584.99	0
0.69	3388.215	2585.01	0.02
0.74	3390	2584.99	0
0	0	2585.01	0.02

Table 10. Negatively Charged

From Table 10 it is seen that no significant mass changes were registered by the scale. Additionally, the very slight mass fluctuations that did occur were not indicative of a weight loss pattern which the machine should have been experiencing with negative charge. Though these results are indicative that the theory behind Yamashita's device does not hold true, an inaccuracy of the machine's dimensions may have been the cause of such results.

A protruding screw, which attached the rotor to the drill chuck, caused a gap of about 2 cm between the top of the rotor to the ceiling of the electrode. This is not in accordance w/ the smaller gap evident from Yamashita's drawings. In addition, the mass of the machine was much greater than the mass of either Vince Berrettini's or Yamashita's. This was mainly due to the additional mass incurred by integrating the fan into the entire assembly of the machine.

When connected to the positive terminal, the machine was accidentally nudged. The scale was allowed to settle and it settled on a new value of 2585.45 g. While connected to the positive terminal, the machine produced the following results presented in Table 11.

Amps	RPM	Mass	Change
0	0	2585.45	0
0.21	1983	2585.45	0
0.24	3087.764	2585.46	0.01
0.29	3254.6	2585.46	0.01
0.34	3319.4	2585.45	0
0.39	3346	2585.44	-0.01
0.44	3364.4	2585.43	-0.02
0.49	3375.2	2585.42	-0.03
0.54	3380.2	2585.45	0
0.59	3384.643	2585.43	-0.02
0.64	3386.429	2585.45	0
0.69	3388.215	2585.44	-0.01
0.74	3390	2585.45	0
0	0	2584.43	-0.02

Table 11. Positively Charged

It is also seen in this case that the machine neither provided a significant mass change or a general increase in mass difference. When continually charged by the Van de Graf generator the machine yielded similar results for both the positively charged and negatively charged case.

Heaviside Force Experiment

The second set of experiments that USAFA conducted was studying the Heaviside force. This research was sponsored under Mr Marc Millis at the NASA Glen Research Center in support of the Breakthrough Propulsion Physics Program. Electromagnetic momentum density is the cross product of the electric field and the magnetic field multiplied by the electric constant. Utilizing Newton's second law, the time derivative of this electromagnetic momentum density is a force density. Utilizing this force density for massless propulsion, generated from independent electric and magnetic fields, is theoretically analyzed and specifically shown that any net thrust, from any configuration, is impossible.

The time derivative of electromagnetic momentum, generated from independent fields, is further analyzed and shown to be a real physical force that accelerates matter independent of the matter's charge. This acceleration of matter, independent of charge, served as motivation behind the possibility that the force is actually the acceleration of space. The speed of the energy flow creating the force is also discussed.

The performed experiment was to determine if this force, created by independent electric and magnetic fields, causes the acceleration of space. A laser interferometer was arranged with one of the laser beams passing through an apparatus that generates

independent and perpendicular electric and magnetic fields. The magnetic field changes periodically in time. If space is accelerated, the interference pattern created by the interferometer will change at the frequency of the changing magnetic field.

The laser interferometer, in this present configuration of field generators, did not find any acceleration of space. Further experiments with different configurations are required and proposed.

Heaviside Experimental Set up



Figure 26. The Heaviside Experiment.

The quartz tube keeps a vacuum on two steel tubes and a copper rod that actually generate the crossed, independent electric and magnetic fields.

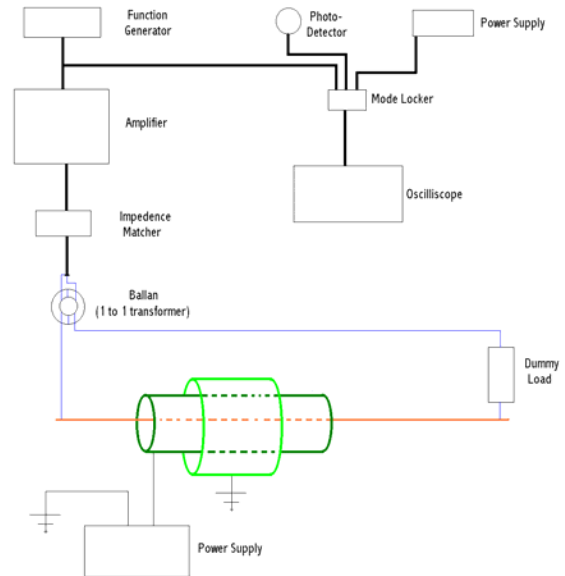


Figure 27. The Electrical Layout.

Two steel tubes, 2 m in length, are used to apply the constant electric field. One tube is placed inside the other with a separation distance of 1 cm. The tubes are separated by Teflon spacers. The tubes are connected to a DC power supply such that the outer tube is grounded and the inner tube is set to a maximum of 12 kV with respect to ground.

Going through the mutual centers of the two tubes is a copper rod 1 cm in diameter. The copper rod is also separated from the inner tube by Teflon spacers. This copper rod will carry an oscillating current which will generate the oscillating magnetic field required to create the proposed force. The two steel tubes and copper rod are incased in a quartz vacuum tube that had a vacuum of 1 μ Torr. At the ends of the quartz tubes are high quality optical windows.

The dimensions of the components were based on what could fit within the quartz tube and what would generate the strongest fields. The voltage limit for the constant voltage power supply were based on the limit of the capacitor. Even though the

constant maximum voltage could be higher theoretically, the capacitor would break down above 12 kV.

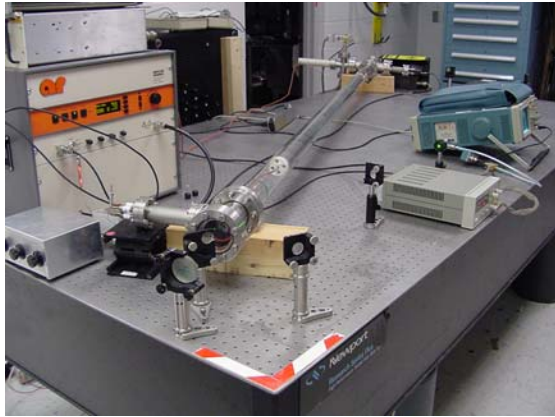


Figure 28. A Closer Quartz Tube View.

Note the optical windows at the end of the quartz tube allow laser light to pass through. Inside the quartz tube are two steel tubes and the copper rod. The white Teflon spacers at the end of the steel tubes separate the tubes and rod. Four holes were drilled into the spacers to allow the laser light to pass.

A 10.03 MHz sinusoid signal, generated by a function generator, is amplified by a RF amplifier. 10.03 MHz was used because it was high enough to produce a reasonable force, around $10\mu\text{N}$, and could be fed through the system without radio waves bouncing back into the amplifier. In the experiment, the amount of amplification is varied. This amplified signal is brought to an impedance matcher and then a ballan. The ballan is a one to one transformer that balances charges on the wires. From the function generator to the ballan, the signal is carried by coaxial cable. After the ballan, transformer wire is used to hook up the ballan to the current feed-throughs on the quartz tube. Coaxial cable is utilized as much as possible to provide electromagnetic shielding. A $50\ \Omega$ dummy load is placed within the circuit. This dummy load is used

because the amplifier is expected to operate with a $50\ \Omega$ load rather than a short circuit.

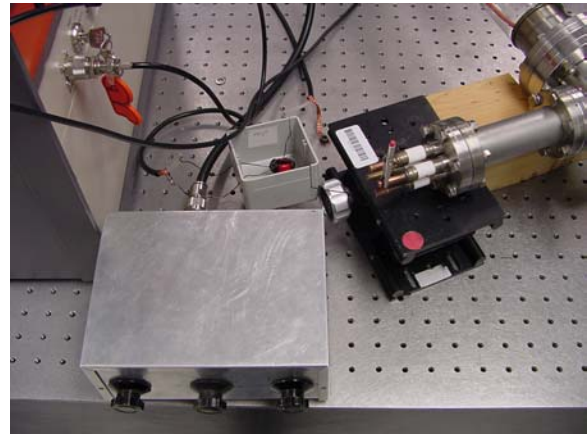


Figure 29. Impedance Matcher and Ballan.

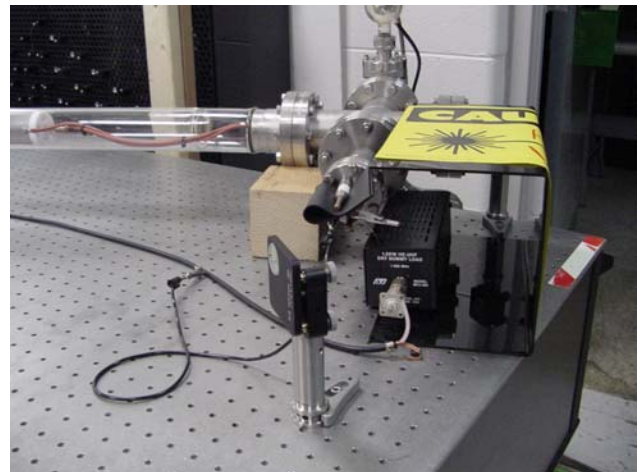


Figure 30. The $50\ \Omega$ Dummy Load.

Figure 29 shows the impedance matcher and ballan. The impedance matcher is the metal box in the lower left hand corner of the table. The ballan, in the center, is the red ferrous toroid that acts as a one to one transformer. Figure 30 shows the $50\ \Omega$ dummy load. It is the black rectangular box near the center.

For the interferometer, a laser beam at 250 nm is split by a beam splitter such that one leg of the laser beam passes between the steel tubes. The laser beams are recombined

and hit a photo detector. The signal from the photo detector is displayed on an oscilloscope. The oscilloscope, however, is locked onto the frequency of the function generator. Therefore, the oscilloscope will only show signals at 10.03 MHz by a DC offset. The idea is that, if space is accelerating, the laser will oscillate at the frequency of the input signal. The oscilloscope will display the laser's oscillation by adding a DC offset to the signal already on oscilloscope. There is a signal already on the oscilloscope because the function generator and amplifier inadvertently emit noisy electromagnetic radiation at the frequency being measured. Thus, there are two modes to this experiment—one with the laser on and one with the laser blocked. If the oscilloscope's signal shows a difference between the two modes, then such an affect would mean the laser is somehow oscillating at 10.03 MHz and would suggest the acceleration of space. Blocking and unblocking the laser was a good method to search for an affect because blocking the signal did not change the electrical properties of the system. Alternatively, the amplifier or voltage source could be turned off or turned down to see if this would modify the signal. However, these methods changed the grounding of the system and gave anomalous results.



Figure 31. The Laser Position.

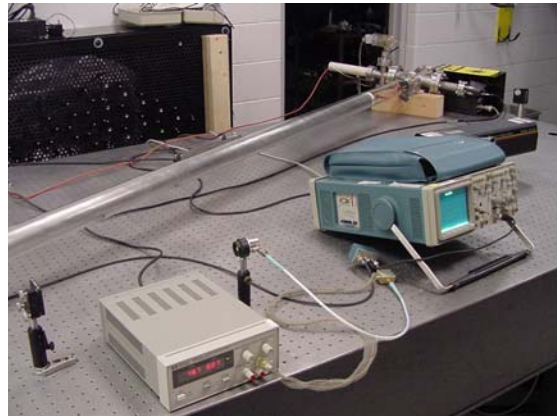


Figure 32. The Photo Detector, Mode Locker, and Oscilloscope.

Figure 31 shows the laser in the center. Figure 32 shows the photo detector, mode locker, and oscilloscope used to measure the magnitude of the 10.03 MHz signal. If space is being accelerated at 10.03 MHz, the oscilloscope's signal will change by a DC drop when the laser beam is physically blocked.

In the experiment, the DC voltage applied to the tubes and the amplification of the current through the wire were measured. These parameters were varied to establish a wide range of experimental data. At each variation, the DC signal from the oscilloscope was read with the laser blocked and without it blocked.

A major concern of the experiment was if the inner steel tube would shield the changing magnetic field. This is because the changing magnetic field would induce a current in the metal tubes that would oppose the current in the rod. Thus, before a measurement was read, the tubes were electrically disconnected from ground and the power supply. This action would greatly limit a current's ability to flow through the tubes. It was verified that the tubes kept

their charge for several minutes once disconnected.

Heaviside Experimental Results

Varying the voltage between the tubes, the power through the rod, and blocking the laser, the following data was collected.

Power from amplifier going into the rod (W)	DC Voltage reading from locked oscilloscope at 10.03 MHz with the Laser ON (mV)	DC Voltage reading from locked oscilloscope at 10.03 MHz with the Laser BLOCKED (mV)
10	10 ± 1	10 ± 1
20	10 ± 1	10 ± 1
30	10 ± 1	10 ± 1
40	7 ± 1	7 ± 1
50	7 ± 1	7 ± 1
60	6 ± 1	6 ± 1

Table 12. Data Collected with 5 kV Between the Steel Tubes.

Power from amplifier going into the rod (W)	DC Voltage reading from locked oscilloscope at 10.03 MHz with the Laser ON (mV)	DC Voltage reading from locked oscilloscope at 10.03 MHz with the Laser BLOCKED (mV)
10	7 ± 1	7 ± 1
20	10 ± 1	10 ± 1
30	6 ± 1	6 ± 1
40	10 ± 1	10 ± 1
50	6 ± 1	6 ± 1
60	6 ± 1	6 ± 1

Table 13. Data Collected with 10 kV Between the Steel Tubes.

Power from amplifier going into the rod (W)	DC Voltage reading from locked oscilloscope at 10.03 MHz with the Laser ON (mV)	DC Voltage reading from locked oscilloscope at 10.03 MHz with the Laser BLOCKED (mV)
10	3 ± 1	3 ± 1
20	4 ± 1	4 ± 1
30	5 ± 1	5 ± 1
40	6 ± 1	6 ± 1
50	6 ± 1	6 ± 1
60	4 ± 1	4 ± 1

Table 14. Data Collected with 12 kV Between the Steel Tubes.

Conclusions

The experiments conducted at the United States Air Force Academy in no way confirmed the existence of an electrogravitational force. Because of the equipment and techniques used, the differences in weight that were actually seen were too statistically insignificant to prove anything. The replica device, however, did not show any evidence contrary to Yamashita's claims. The first claim, that a horizontal rotating body produces a vertical force, could not be disproved. The spinning rotor and its effect on the replica device's weight did not disprove the first claim by virtue of the fact that the data needed to prove or disprove this claim was statistically insignificant. Another one of Yamashita's claims, that reversing the polarity should reverse the direction of the force, could not be disproved, for the same reason. The device seemed to generally decrease its weight when given a negative charge, and increase its weight with a positive charge, again however, this weight change was not statistically conclusive. The final claim that

could not be rebuked is that the magnitude of the force generated increases with the speed of rotation of the charged body. One can see from the tables that this did tend to happen, although again statistically insignificant. Yamashita's fourth claim, that a force could be produced in any direction, was not observed in this experiment.

In order to be able to prove or disprove Yamashita's claims, it would be absolutely necessary to know exactly what he did in his experiment. Unfortunately, the ambiguity of his patent left a lot of room for guesswork. A number of assumptions were made in the absence of information from Yamashita's patent. These assumptions may be partly responsible for the fact that this experiment did not produce any conclusive results.

This experiment neither denied, nor definitely confirmed the existence of an electrogravitational force. Conclusive proof or disproof would require better data than that collected from this experiment.

Similar results were obtained in the Heaviside force experiment. As shown in the data above, there is no difference between the oscilloscope signals between when the laser is on or it is blocked. Although not shown here, it was determined that the accuracy of the interferometer was 1 in 10^{18} . Thus, it may be concluded space is not being accelerated at 10.03 MHz.

This team later discovered, however, this configuration of electric and magnetic fields may not give rise to acceleration. One of the big questions asked by this team is that if space is being accelerated, what is the procedure to calculate the acceleration. Only after building the experiment, was a satisfying method of calculating acceleration established using Poynting's theorem. The calculated speed, had for its denominator the

dot product between the applied constant electric field and the induced electric field. In this configuration, the applied electric field and induced electric field are perpendicular. Resultantly, the calculation for speed would have a zero in the denominator and hence velocity and acceleration, in this configuration, would not make sense. Thus, a new experiment, with the fields oriented in a new manner, may be in order.

Based on the speed expression, a new device, as shown in Figure 33, could be developed where the applied electric field is parallel to the induced electric field. In this configuration, the force would exist between the capacitor plates and oscillate in the radial direction. That way, the expression for v may make more physical sense and, consequentially, the acceleration may be detectable.

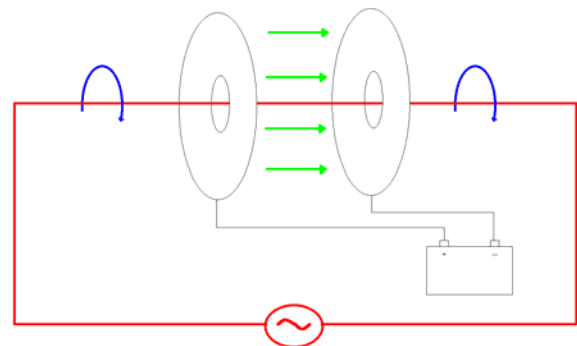


Figure 33. Parallel Plate Capacitor Configuration.

As illustrated in Figure 33, instead of cylindrical capacitors, parallel plate capacitors could be utilized. This way, the induced electric field is parallel to the applied electric field and, resultantly, the concept of velocity and acceleration makes more sense in this configuration.

In addition, to verify that this force actually affects matter, piezo- electric ceramic strips

could be utilized to detect the force. In the device in Figure 33, the peizo- electric strips would be assembled around the wire between the capacitor plates. The peizo- electric strips, having a thickness of about 8 mm, have a natural resonant frequency of about 8 MHz along the thickness. The radial, but oscillating force, produced by the new device, would be tuned to also oscillate 8 MHz. The result, if the force really exists, would be the strong oscillation of the peizo- electric strips which, when combined together, would produce a detectable signal. This experiment would differ from Graham's experiment in that his team detected electromagnetic angular momentum, whereas this experiment would detect electromagnetic linear momentum.

We feel these experiments were successful though, since finding these concepts not significant and worthy of further research in the field of Breakthrough Propulsion Physics for NASA, resources can be allocated to investigate other concepts.

References

1. Yamashita, H., et. al., *Machine for Acceleration in a Gravitational Field*. European Patent 0486243A2, 1991.

2. Rognerud, Nils, *Free Fall of Elementary Particles: On Moving Bodies and their Electromagnetic Forces*, 1994.

3. Xylene: Material Safety Data Sheet. Sep. 99. CHEM-SUPPLY Pty Ltd, Gillman, South Africa.

4. Schlagheck, Christopher. *Weight Loss Effects Associated with a Rotating Charged Cylinder*. 2002.

5. Berrettini, Vincent., *The Coupling of Mass and Charge as a Propulsive Mechanism*, 2004.

6. Rognerud, Nils, *Free Fall of Elementary Particles: On Moving Bodies and their Electromagnetic Forces*, 1994.

7. Tajmar, M. and de Matos, C. J., *Introduction and Amplification of Non-Newtonian Gravitational Fields*, 2001.

8. Corum, J., "The electromagnetic stress tensor as a possible space drive propulsion concept," *AIAA Journal of Propulsion and Power*, 2001.

9. Graham, G., "Observation of static electromagnetic angular momentum in vacuo," *Nature*, Vol. 285, No. 576, 15 May 1980, pp. 154- 155.

10. Slepian, J., "Electromagnetic Space-Ship," *Electrical Engineering*, January 1949, pp. 145- 146.

11. Wertz, J. R., Wiley, J. L., *Space Mission Analysis and Design*, Microcosm Press, 1999

12. Humble, W. H., Henry, G. N., Wiley, J.L.; *Space Propulsion Analysis and Design*, McGraw-Hill Company, 1995

13. Angelo, Joseph A. Jr., and Buden, David, *Space Nuclear Power*, Orbit Book Company, 1985.